Published in final edited form as:
Curr Biol. 2009 June 23; 19(12): 996–1004. doi:10.1016/j.cub.2009.05.043.

Lateralized gustatory behavior of *C. elegans* is controlled by specific receptor-type guanylyl cyclases

Christopher O. Ortiz[1], **Serge Faumont**[2], **Jun Takayama**[3], **Heidi K. Ahmed**[1], **Andrew D. Goldsmith**[1], **Roger Pocock**[1], **Kathryn E. McCormick**[2], **Hirofumi Kunimoto**[3], **Yuichi Iino**[3,4], **Shawn Lockery**[2], and **Oliver Hobert**[1,§]

[1]Howard Hughes Medical Institute, Department of Biochemistry and Molecular Biophysics, Columbia University Medical Center, New York, NY 10032

[2]Institute of Neuroscience, University of Oregon, Eugene, OR 97403

[3]Department of Biophysics and Biochemistry, University of Tokyo Bunkyo-ku, Tokyo 113-0033, Japan

[4]Molecular Genetics Research Laboratory and Graduate School of Science, University of Tokyo Bunkyo-ku, Tokyo 113-0033, Japan

SUMMARY

Background—Even though functional lateralization is a predominant feature of many nervous systems, it is poorly understood how lateralized neural function is linked to lateralized gene activity. A bilaterally symmetric pair of gustatory neurons in the nematode *C. elegans*, ASEL and ASER, serves as a model to study the genetic basis of functional lateralization as this pair senses a number of chemicals in a left/right asymmetric manner. The extent of functional lateralization of the ASE neurons and genes responsible for the left/right asymmetric activity of ASEL/R are unknown.

Results—We show here that a large panel of salt ions is sensed in a left/right asymmetric manner, as demonstrated by behavioral assays, imaging of neural activity with a genetically encoded calcium sensor and by genetic manipulations that alter the fate of either ASEL or ASER. We show that lateralized salt responses allow the worm to discriminate between distinct salt cues. To identify molecules that may be involved in sensing salt ions and/or transmitting such sensory information, we examined the chemotaxis behavior of animals harboring mutations in eight different receptor-type, transmembrane guanylyl cyclases (encoded by *gcy* genes), which are expressed in either ASEL (*gcy-6*, *gcy-7*, *gcy-14*), ASER (*gcy-1*, *gcy-4*, *gcy-5*, *gcy-22*) or ASEL and ASER (*gcy-19*). Disruption of a ASER-expressed *gcy* gene, *gcy-22*, resulted in a broad chemotaxis defect to nearly all salts sensed by ASER, as well as to a left/right-asymmetrically sensed amino acid. In contrast, disruption of other *gcy* genes resulted in highly salt ion-specific chemosensory defects. Furthermore, we show that not only the cyclase domain, but also the extracellular domain of GCY proteins is important for their activity in salt sensation.

Conclusions—Our findings broaden our understanding of lateralities in neural function, provide insights into how this laterality is molecularly encoded and reveal an unusually diverse spectrum of signaling molecules involved in gustatory signal transduction.

§Corresponding author: Columbia University, 701 W. 168th Street, HHSC 724, New York, NY. E-mail: or38@columbia.edu.

INTRODUCTION

Functional lateralization is a poorly understood feature of many nervous systems [1]. Few if any molecules are known to be asymmetrically expressed in functionally lateralized areas in the brain of higher vertebrates [2]. The nervous system of the nematode *C. elegans* also displays functional lateralization, and in this case, several molecular correlates to functional lateralization exist in the form of putative chemoreceptor molecules [3]. One example is the ASE gustatory neuron class, which is made up of two neurons that are morphologically symmetric, ASE-left (ASEL) and ASE-right (ASER)(Fig.1A). This neuron pair serves as the main sensor for multiple types of taste cues [4]. Although anatomically largely symmetric, ASEL and ASER are functionally asymmetric in the way they respond to salts; ASEL is primarily required for attracting worms to Na^+ and ASER for attraction to Cl^- and K^+ [5]. Moreover, ASEL is an "ON-cell" that is activated by increasing concentrations of NaCl, whereas ASER is an "OFF-cell" that is activated by decreasing concentrations of NaCl [6]. The "ON-cell" induces "run" behavior toward a sensory cue, whereas the "OFF-cell" induces "turn" behavior.

Neither the extent of the functional lateralization of ASEL/R, nor the molecular basis for the asymmetric responses to salt ions are well characterized. In fact, signal transduction pathways that mediate an animal's gustatory response to salt ions are generally poorly understood in any system to date [7]. Previous gene expression analysis has revealed that the lateralized ASE neurons coexpress a large number of receptor-type guanylyl cyclases (rGC) in a left/right asymmetric manner [8,9](Fig.1A). rGCs are composed of a large N-terminal extracellular domain, a transmembrane domain, an inactive protein-kinase like regulatory domain, and a guanylyl cyclase domain [10](Fig.1B). The role of rGCs in gustatory behavior has, however, remained largely unexplored so far. Here, we show that several rGCs have specific functions in mediating the response to individual salt ions, including previously identified and newly identified left/right asymmetrically sensed chemoattractants. Our study makes rGC proteins the first molecules shown to be directly responsible for lateralized neuron function and provides novel insights into the diverse nature of signal transduction mechanisms triggered by salt ions.

RESULTS

A panel of salt taste cues is sensed by ASEL/R in a left/right asymmetric manner

Despite the diversity of molecules *C. elegans* likely encounters in its native soil habitat, the number of chemicals identified as chemoattractants is relatively small, many of the previously identified chemoattractants have not been completely mapped to individual sensory neurons and little is known about how many chemosensory cues are sensed in a left/right asymmetric manner. Moreover, the classic study that identified attractive salt cues for *C. elegans* tested responses to salt ions paired with what were considered "neutral" counterions, ammonium and acetate [11]. However, recent work revealed that those are in fact attractive cues under specific assay conditions [12], therefore warranting a re-evaluation of salt ion responses. For this re-evaluation, we minimized the chemotactic response to the ammonium and acetate counterions by modifying previous assay conditions through including a saturating background of ammonium acetate in the assay plate (Supp.Fig.S1; Experimental Procedures). With these novel assay conditions in hand, we first addressed whether various salt ions previously thought to be attractive to worms are indeed attractive with the impact of the counterion minimized and are sensed by the ASE gustatory neuron, one of several gustatory neurons in the *C. elegans* head. To test for ASE involvement, we examined the behavior of wild-type and *che-1 (ot66)* mutant animals in gradients of Mg^{2+}, Li^+, Br^- and I^- ions. *che-1* encodes a C2H2-type zinc finger transcription factor that is required for the appropriate development of ASE [13]. c*he-1* animals displayed profound defects in their ability to chemotax to Mg^{2+}, Li^+, Br^- and I^- compared to wild-type, suggesting that ASE is the primary chemosensory cell pair required

for detection of these ions (Fig.1D). Overall locomotion and response to olfactory cues are not affected in *che-1* mutant animals [14].

Previous work demonstrated that ASEL and ASER contribute differentially to an animal's response to Na^+, K^+ and Cl^- [5,6]. To determine if ASEL and ASER are also differentially required for chemotaxis to Mg^{2+}, Li^+, Br^-, and I^-, we assessed the ability of animals with genetically or microsurgically ablated ASEL or ASER neurons (see Experimental Procedures) to migrate up gradients of these ions. We find that Br^- and I^- chemotaxis requires ASER, but not ASEL, while Mg^{2+} and Li^+ chemotaxis primarily depends on ASEL, but not ASER (Fig. 1D, Suppl. Fig.S2). Lateralized chemotaxis is not restricted to salt responses; the amino acid methionine is also sensed in a left/right asymmetric manner by the ASER neuron (Suppl. Fig.S3).

We furthermore visualized this lateralized behavioral response to salt using the genetically encoded calcium sensor cameleon [15]. Previous work using this technique demonstrated that ASEL responds preferentially to upsteps of NaCl concentration, whereas ASER responds preferentially to downsteps in salt concentration [6]. In contrast to this previous study, we did not assay the response to two paired ions (NaCl) that simultaneously activate ASEL and ASER, but rather imaged the calcium response of ASEL and ASER to individual ions. As in the behavioral assay, this was achieved by pairing individual ions with ammonium or acetate and assaying calcium responses in a background of saturating ammonium acetate (see Experimental Procedures; under these conditions, ammonium acetate can not evoke an ASE response; Fig. 2A). We find that intracellular calcium levels in ASEL show a larger and faster response to Na^+ upsteps, compared to the response seen in ASER during Na^+ downsteps (Fig.2A; see Supp.Fig.S4 for comparison of ASEL vs. ASER response to all tested cues). Similarly, and consistent with behavioral and ablation data, ASEL also responds robustly to Mg^{2+} and Li^+ upsteps, whereas ASER responds weakly if at all to both upsteps and downsteps. In contrast, intracellular calcium levels in ASER show a larger and faster response to downsteps in Cl^- concentration, compared to the response seen in ASEL during a Cl^- upstep (Fig. 2A;Suppl.Fig.S4). Similarly, and again consistent with behavioral and ablation data, ASER displays a strong response to Br^- and I^- downsteps, whereas ASEL responds weakly to upsteps and downsteps. In addition to increases in calcium levels, in some cases ASER responds to upsteps of some cues with a decrease in intracellular calcium compared to baseline (Fig.2A). In the case of K^+, calcium imaging shows that both ASEL and ASER show significant responses to K^+, one to an upstep, the other to a downstep (Fig.2A;Suppl.Fig.S4). Given that ablation analysis indicates that only ablation of ASER but not ASEL decreased attraction to K^+ [5], the ASER response appears functionally more relevant than the ASEL response.

We next asked whether the lateralized ability to sense individual salt ions allows the animal to discriminate between different salt cues. To address this question, we performed discrimination assays, in which the ability of animals to migrate up a gradient of one salt in a saturating background concentration of another salt is tested (Fig.2B). We find that animals can distinguish between ASEL-sensed cues and ASER-sensed cues, but they cannot distinguish individual ASEL or ASER-sensed cues from one another; that is, for example, animals can sense Br^-(ASER-sensed) in the presence of Li^+ (ASEL-sensed) but not in the presence of I^- (ASER-sensed)(Fig.2B) These results corroborate the previously made notion [5,11] that lateralization serves to broaden the ability of a worm to navigate in complex sensory environments.

Reprogramming ASE response profiles in developmental, left/right asymmetry mutants

ASEL and ASER identity, as assessed by the expression of receptor-type guanylyl cyclases, can be manipulated through specific genetic manipulations. The miRNA *lsy-6* is normally expressed in ASEL where it promotes ASEL fate and represses ASER fate such that loss of

lsy-6 results in the adoption of a 100% penetrant "2-ASER" state [16]. In contrast, forced expression of *lsy-6* in ASER (using the *otIs204* transgene), results in a 100% penetrant "2-ASEL" state [16]. We imaged calcium responses in both "2-ASER" and "2-ASEL" animals to test how symmetrizing ASE identity correlates with the responsiveness to sensory cues. We find that calcium profiles perfectly track with cell identity. In addition to adopting the preferential ion sensitivities of the transformed cell fate, the transformed neurons also adopt the OFF-cell and ON-cell sensitivities seen in the respective wild-type neurons. In "2-ASER" animals, the ASEL neuron now transforms into an "OFF neuron", whereas in "2-ASEL" animals the ASER neuron transforms into an "ON neuron" (Fig.3A). The amplitude and waveform of the calcium traces also show a remarkable agreement between true and transformed neurons.

The transformation in calcium profiles also produces transformation in behavioral outputs. "2-ASER" mutants are still attracted to all ASER sensed cues (Cl^-, Br^-, I^-, K^+), yet their response to all ASEL sensed cues (Na^+, Li^+, Mg^{2+}) is significantly impaired (Fig.3B). "2-ASEL" animals are still attracted to all ASEL-sensed cues and show either an impaired (Cl^- and K^+) or even inverted response (Br^- and I^-) to ASER cues (Fig.3B). This pattern of salt taste responsiveness is consistent with the asymmetric responsiveness suggested by the ASE ablation experiments above and, moreover, demonstrate that "ON" and "OFF" responses to a sensory cue are alone sufficient to drive behavior.

gcy genes are required for chemotaxis to specific sets of salt taste cues

To identify the molecular basis of lateralized salt responsiveness, we examined in salt chemotaxis assays mutant animals carrying deletion alleles that impair or eliminate ASEL- and/or ASER-expressed receptor-type guanylyl cyclases, encoded by the *gcy* genes (Fig.4A; see Experimental Procedures). Mutant responses fell into one of three categories (Fig.4A): severe chemotaxis defects to nearly all cues tested (*gcy-22*); significant chemotaxis defects to a subset of salt taste cues while retaining full responsiveness to others (*gcy-1*, *gcy-4*, *gcy-6*, *gcy-14*); or no chemotaxis defects to any of the salts tested (*gcy-5*, *gcy-7*, *gcy-19*; those may be involved in mediating the response to other salt ions not tested in this study). For all cases in which a chemotaxis defect was identified, a genomic copy of the wild-type gene was found to restore full attraction to the affected cues (Supp. Fig.S5–S7).

gcy-22 mutants display broad chemotaxis defects

Expression of *gcy-22* is restricted to ASER as assessed by reporter gene analysis using a promoter fusion [17], as well as a genomic fosmid clone, in which we engineered *gfp* into the *gcy-22* locus (data not shown). The *tm2364* allele contains an out of frame deletion that introduces an early stop signal, and is thus a likely molecular null (Fig.4A). Analysis of the chemotaxis response of *gcy-22* animals reveals that they display significantly weaker attraction to all salts tested, with the exception of ASEL-sensed Na^+ (Fig.4A). *gcy-22* is also required for a response of animals to the amino acid methionine, which is primarily sensed by the ASER neuron (Suppl.Fig.S3). Moreover, consistent with a critical role for *gcy-22* in triggering neural activity in ASER, we also find that the ASER neurons display aberrant axonal sprouts (Suppl.Fig.S3). Such defects are indicative of neuronal activity defects, as they can also be observed upon elimination of other molecules involved in generating neuronal activity, such as the cGMP-gated *tax-2/tax-4* ion channels [18]. Even though broad, the sensory deficits of *gcy-22* are limited to ASE-sensed cues and are not a mere reflection of, for example, locomotory defects as odortaxis to a point source of the AWC-sensed odorant benzaldehyde is similar to the wild-type response (data not shown).

Chemotaxis defects toward ASER-sensed salts can be rescued through ASER-, but not ASEL-specific expression of *gcy-22* in transgenic animals (Suppl.Fig.S5), consistent with the ASER-

specific expression of *gcy-22*. This transgenic rescue assay also allowed us to undertake structure/function analysis of GCY-22. Mutational analyses demonstrate that both the extracellular, intracellular and guanylyl cyclase domain are required for GCY-22 function (Supp.Fig.S5); moreover, the extracellular domain of GCY-22 cannot be replaced by the extracellular domain of another GCY protein, ODR-1, underscoring the specificity of extracellular domain function.

gcy-1, gcy-4, gcy-6 and *gcy-14* mutants display salt-specific chemotaxis defects

In contrast to *gcy-22* mutants, animals carrying mutations in other ASER-expressed *gcy* genes showed defects that were more selective for individual, laterally sensed salt ions. The *gcy-1 (tm2669)* allele contains an out-of-frame deletion spanning from the fourth exon through the seventh intron and is thus expected to be a molecular null (Fig.4A). Animals homozygous for this allele can migrate up gradients of all salts as efficiently as wild-type animals, except for ASER-sensed K^+ toward which *gcy-1* mutant animals show no response (Fig.4A). This ASER-specific sensory defect is consistent with the ASER-specific expression of *gcy-1* [9]. ASER-specific expression of a wild-type copy of *gcy-1* controlled by the *gcy-5* promoter in a *gcy-1* mutant background restores responsiveness to K^+ while ASEL-specific expression fails to restore responsiveness to K^+ (Suppl. Fig.S6), thereby corroborating that *gcy-1* acts in ASER to promote K^+ chemotaxis.

Animals with a mutation in the ASER-biased gene *gcy-4* show a set of salt-selective defects that are complementary to those seen in *gcy-1* mutants; they respond normally to K^+ (data not shown) and show chemotaxis defects exclusively on gradients of Br^- and I^- (Fig.4A). The same upstream regulatory region of *gcy-4* that drives reporter gene expression in ASER rescues the *gcy-4* mutant phenotype when driving a genomic copy of the *gcy-4* locus (Supp. Fig.S6). The residual response to Br^- and I^- of animals lacking the ASER-expressed *gcy-4* is further enhanced in a *gcy-4; gcy-22* double mutant background (Supp.Fig.S8). Since rGCs act as dimers [10], this enhancement data may suggest a model in which GCY-4 and GCY-22 encode the subunits of a heterodimeric complex, with each homodimer retaining residual function.

Salt-specific defects can also be found upon elimination of *gcy* genes whose expression is biased toward or exclusive to ASEL. A *gcy-14* mutant strain displays a significantly weaker response to ASEL-sensed Na^+ and Li^+ gradients, but normal responses to other salts (Fig.4A). ASEL-specific expression fully rescues the Na^+ chemotaxis defect of *gcy-14* mutants, whereas ASER specific expression does not (Suppl.Fig.S7). As with the ASER-expressed GCY-22 protein, GCY-14 also requires both its extracellular and intracellular domain for function (Supp. Fig.S7). We conclude that *gcy-14* acts in ASEL to mediate the chemotaxis response to ASEL-sensed Na^+ and Li^+.

Animals carrying a mutation in the ASEL-expressed *gcy-6* gene also display a highly salt-specific chemotaxis phenotype. While chemotaxis to most of the panel of ions tested was indistinguishable from wild-type, these animals showed a dramatic decrease in their ability to respond to an ASEL-sensed Mg^{2+} gradient, consistent with the ASEL-specific expression of *gcy-6* (Fig.4A). Combining *gcy-6* with *gcy-7* mutants (in which no defects were observed) did not reveal any defects for ASEL-sensed cues beyond these seen for *gcy-6* alone (Fig.4A).

Imaging neuronal activity in *gcy* mutants

The ASE neurons require the cGMP-gated cation channels TAX-2/TAX-4 to produce calcium currents required for ASE-mediated chemotaxis [6,19,20]. To test whether cGMP-producing GCY proteins are involved in generating these calcium currents, we performed calcium imaging of animals mutant for either an ASEL-expressed *gcy* gene (*gcy-6*) or an ASER-expressed *gcy* gene (*gcy-22*) using the cameleon sensor. We find that the salt-selective

behavioral defects of *gcy-6* mutants are perfectly mirrored by the calcium imaging data; calcium responses to Mg^{2+} and, to a more limited extent Cl^{-}, are affected in *gcy-6* animals, while responses to other ions are unaffected (Fig.4B). Again consistent with behavioral assays, we detect broad defects in calcium responses of ASEL and ASER of *gcy-22* mutant animals (Supp. Fig.S9). GCY proteins are therefore upstream inducers of lateralized neuronal activity.

DISCUSSION

The studies described here broaden our understanding of the functional laterality in the nematode gustatory system and provide insights into how this laterality is molecularly encoded. Our behavioral examination of animals in which either ASEL or ASER are ablated and our calcium imaging studies reveal that a wide spectrum of distinct ions is sensed in a left/right asymmetric manner by the ASEL and ASER neurons (Fig.5). The overall purpose of such lateralization is that it endows the animal with the ability to discriminate between different salt ions.

The cellular response profiles to the salt ions tested in this paper are consistent with and extend previous findings which demonstrated that ASER neuron generally responds to a downstep in the concentration of a sensory cue, whereas the ASEL neuron responds to an upstep [6]. We further extended these previous findings, which were undertaken with a salt that induces responses in both ASEL and ASER (NaCl), by showing that activation of either cell alone (*e.g*. ASEL by Na^{+} or ASER by Cl^{-}) is sufficient to produce an efficient chemotactic response. That is, animals appear to be able to migrate toward an ASER-sensed cue solely by being repelled by downsteps in a concentration gradient, which induces a turning response and thereby guides the animal upwards on a concentration gradient. The sufficiency of “ON” or “OFF” neurons to produce effective responses to salt ions is further corroborated by our use of genetically transformed “2-ASER” and “2 ASEL” animals. The genetic transformation studies also make the point that the “ON” and “OFF” responses are an intrinsic and cell-autonomous property of the two neurons rather than an overall circuit property.

Our mutant analysis of asymmetrically expressed *gcy* genes demonstrates that the asymmetric expression of chemosensory signaling molecules underlies the asymmetric ion sensitivities of ASEL and ASER. The ion selectivity of GCY protein function is notable and demonstrates that there is no common anion- or cation-induced signaling pathway (Fig.5). In striking contrast, one GCY protein, ASER-expressed GCY-22, is defective in responding to all ASER-sensed cues. Since rGCs are generally thought to act as dimers [21], these findings suggest a model, to be tested in future studies, in which GCY-22 may be a common subunit of several more ion-selective heterodimeric complexes.

Transmembrane, receptor-type GCY proteins are receptors for small peptide ligands in vertebrates [10]. The presence and conservation of the extracellular domains of worm rGC proteins, as well as their localization to the sensory apparatus in dendritic endings of sensory neurons, is consistent with a role for GCY proteins in being salt-regulated receptor proteins. A direct salt receptor role for rGC proteins is also suggested by the finding that the extracellular domain of the ANP receptor, a rGC, contains a conserved chloride-binding site and that hormone binding and ensuing receptor activation is chloride dependent [22]. Moreover, a chimeric protein consisting of the extracellular domain of a mammalian rGC and the intracellular domain of *C. elegans gcy-28* exhibited cyclase activity upon binding a peptide ligand known to activate the mammalian rGC [23], demonstrating that the GC domain of *C. elegans* rGC proteins is ligand-responsive. Alternatively, rather than acting as direct receptors, specific rGC complexes may be selectively coupled to other ion-selective receptor proteins. But no matter whether GCY proteins are direct receptors or downstream signaling components it is surprising and unusual to have distributed an apparently single enzymatic function – the

production of cGMP for gating the downstream TAX-2/4 channels – over several molecules, each apparently dedicated to selectively transmitting different sensory inputs.

EXPERIMENTAL PROCEDURES

A list of strains, transgenes and details on standard molecular biological procedures can be found in the Supplementary Material.

Chemotaxis Assays

The response to salt gradients was assayed as previously described [24], with some modifications. Buffered agar (20 g/L agar, 1 mM $CaCl_2$, 1 mM $MgSO_4$, 5 mM KPO_4) was supplemented with 100 mM NH_4Ac to saturate for NH_4^+ and Ac^- responses (we confirmed that ASE was unresponsive to NH_4Ac gradients under these conditions; Supp.Fig.S1); 10 mL of this was poured into 10 cm diameter Petri dishes. To establish the gradient, 12–16 hours before assay, 10 μL of 2.5 M salt solutions adjusted to pH = 6 with either NH_4OH or acetic acid was applied to the attractant spot, while 10 μL of ddH_2O was applied to the control spot. Another 4 μL of salt solution or water was added to the same spots 4 hours before assay. 10 minutes before assay a 2 μL drop of 1 M sodium azide was applied to both attractant and control spots to immobilize worms that reached these areas. Synchronized adult animals were washed twice with CTX solution (1 mM $CaCl_2$, 1 mM $MgSO_4$, 5 mM KPO_4) and 100–200 were placed in the center of the assay plate in a minimal volume of buffer. A kimwipe was used to wick away buffer and animals were allowed to move about the agar surface for one hour, after which assay plates were placed at 4°C overnight. The distribution of animals across the plate was then determined and a chemotaxis index was calculated according to the diagram in Fig.1C. Salt discrimination assays were done in same manner but the 100 mM NH_4Ac background was replaced with a 50 or 100 mM background of a particular salt. Methionine quadrant chemotaxis assay was done as depicted in Supp. Fig.S6.

Calcium Imaging

Young adult animals were transferred in liquid to an agarose-coated coverslip (2% agarose in TAPS 30 mM, pH 9), anesthetized by cooling, and glued to the coverslip with cyanoacrylate glue (Nexaband Quick Seal, Veterinary Products Laboratory, Phoenix, AZ, USA). The nose of each animal was placed in close proximity (~0.5 mm) to a two-channel gravity-fed perfusion pencil whose flow was controlled by programmable upstream valves (AutoMate Scientific, Berkeley, CA, USA). Solutions contained the indicated concentration of tested ions (usually 50 mM), plus (in mM): phosphate buffer (5), $CaCl_2$ (1), $MgSO_4$ (1), ammonium acetate (100); osmolarity was adjusted to 350 mOsm with sorbitol. The buffer bath with100 mM NH_4Ac replicates conditions used in the population chemotaxis assays and eliminates the contribution of the NH_4^+ and Ac^- counterions on chemotaxis. We confirmed that ASE was unresponsive to 50 mM steps of NH_4Ac under these conditions. Optical recordings were performed on a Zeiss Axiovert 135, using a Zeiss Plan-Apochromat 63×oil, 1.4 NA objective. The microscope was equipped with an epifluorescence illuminator, software-controlled shutter (ASI, Eugene, OR, USA), beam splitter (Optical Insights, OI-DV-FC, Tucson, AZ, USA) and digital video camera (Hamamatsu, ORCA-AG, Bridgewater, NJ, USA). Images were acquired using the MetaVue software (version 6.2r2, Molecular Devices, Sunnyvale, CA). Frames were taken at a ~10 to 20 Hz with 8×8 spatial binning. A TTL pulse was used to synchronize image acquisition and the timing of solution switching. Image stacks were processed using Jamlyze (written by Rex Kerr, HHMI Janelia Farms), and data then imported into Igor (Wavemetrics, Lake Oswego, OR) for further analysis. The YFP/CFP emission ratio was computed as (YFP intensity)/(CFP intensity) − 0.65, where the latter term corrects for CFP bleed-through into the YFP channel. The emission ratio was compensated for photobleaching by fitting a single exponential function to the inactive portions of the emission ratio trace, and dividing it by the

fitted curve; thus, all ratio changes were expressed in terms of *DR*/*R*. Individual traces were interpolated to a 100 Hz sampling rate and averaged.

Statistical Analysis

Statistical tests were done using Microsoft Excel Data Analysis software. Values for all behavioral assays are reported as the mean ± standard error of the mean (SEM). Comparisons between experimental values and controls were made using a two-sample Student's t-test assuming equal variance, and two-tailed P values were used. In datasets for which multiple t-tests were done, the Bonferroni correction was applied.

Supplementary Material

Refer to Web version on PubMed Central for supplementary material.

ACKNOWLEDGEMENTS

We thank Q. Chen for expert DNA injection, M. Sotodate for assistance with building the UV/TMP mutagenized library, T. Tanaka for mutant library PCR screening, the CGC for providing strains, members of the Hobert lab for discussion and comments on the manuscript and Shohei Mitani at Tokyo Women's Medical University School of Medicine for knockout alleles. This work was supported by the National Institutes of Health (NIH) Medical Scientist Training Program and an NIH predoctoral fellowship (F31DC009098-01) to C.O.O. O.H. acknowledges funding by the NIH (R01NS039996-05; R01NS050266-03). O.H. is an Investigator of the HHMI.

References

1. Davidson, RJ.; Hugdahl, K., editors. Brain Asymmetry. Cambridge, MA: MIT Press; 1994.
2. Sun T, Walsh CA. Molecular approaches to brain asymmetry and handedness. Nat Rev Neurosci 2006;7:655–662. [PubMed: 16858393]
3. Hobert O, Johnston RJ Jr, Chang S. Left-right asymmetry in the nervous system: the Caenorhabditis elegans model. Nat Rev Neurosci 2002;3:629–640. [PubMed: 12154364]
4. Bargmann CI, Horvitz HR. Chemosensory neurons with overlapping functions direct chemotaxis to multiple chemicals in C. elegans. Neuron 1991;7:729–742. [PubMed: 1660283]
5. Pierce-Shimomura JT, Faumont S, Gaston MR, Pearson BJ, Lockery SR. The homeobox gene lim-6 is required for distinct chemosensory representations in C. elegans. Nature 2001;410:694–698. [PubMed: 11287956]
6. Suzuki H, Thiele TR, Faumont S, Ezcurra M, Lockery SR, Schafer WR. Functional asymmetry in Caenorhabditis elegans taste neurons and its computational role in chemotaxis. Nature 2008;454:114–117. [PubMed: 18596810]
7. Scott K. Taste recognition: food for thought. Neuron 2005;48:455–464. [PubMed: 16269362]
8. Yu S, Avery L, Baude E, Garbers DL. Guanylyl cyclase expression in specific sensory neurons: a new family of chemosensory receptors. Proc Natl Acad Sci U S A 1997;94:3384–3387. [PubMed: 9096403]
9. Ortiz CO, Etchberger JF, Posy SL, Frokjaer-Jensen C, Lockery S, Honig B, Hobert O. Searching for neuronal left/right asymmetry: genomewide analysis of nematode receptor-type guanylyl cyclases. Genetics 2006;173:131–149. [PubMed: 16547101]
10. Lucas KA, Pitari GM, Kazerounian S, Ruiz-Stewart I, Park J, Schulz S, Chepenik KP, Waldman SA. Guanylyl cyclases and signaling by cyclic GMP. Pharmacol Rev 2000;52:375–414. [PubMed: 10977868]
11. Ward S. Chemotaxis by the nematode Caenorhabditis elegans: identification of attractants and analysis of the response by use of mutants. Proc Natl Acad Sci U S A 1973;70:817–821. [PubMed: 4351805]
12. Frokjaer-Jensen C, Ailion M, Lockery SR. Ammonium-acetate is sensed by gustatory and olfactory neurons in Caenorhabditis elegans. PLoS ONE 2008;3:e2467. [PubMed: 18560547]

13. Etchberger JF, Lorch A, Sleumer MC, Zapf R, Jones SJ, Marra MA, Holt RA, Moerman DG, Hobert O. The molecular signature and cis-regulatory architecture of a C. elegans gustatory neuron. Genes Dev 2007;21:1653–1674. [PubMed: 17606643]

14. Law E, Nuttley WM, van der Kooy D. Contextual taste cues modulate olfactory learning in C. elegans by an occasion-setting mechanism. Curr Biol 2004;14:1303–1308. [PubMed: 15268863]

15. Miyawaki A, Llopis J, Heim R, McCaffery JM, Adams JA, Ikura M, Tsien RY. Fluorescent indicators for Ca2+ based on green fluorescent proteins and calmodulin. Nature 1997;388:882–887. [PubMed: 9278050]

16. Johnston RJ, Hobert O. A microRNA controlling left/right neuronal asymmetry in Caenorhabditis elegans. Nature 2003;426:845–849. [PubMed: 14685240]

17. Johnston RJ Jr, Chang S, Etchberger JF, Ortiz CO, Hobert O. MicroRNAs acting in a double-negative feedback loop to control a neuronal cell fate decision. Proc Natl Acad Sci U S A 2005;102:12449–12454. [PubMed: 16099833]

18. Peckol EL, Troemel ER, Bargmann CI. Sensory experience and sensory activity regulate chemosensory receptor gene expression in Caenorhabditis elegans. Proc Natl Acad Sci U S A 2001;98:11032–11038. [PubMed: 11572964]

19. Coburn CM, Bargmann CI. A putative cyclic nucleotide-gated channel is required for sensory development and function in C. elegans. Neuron 1996;17:695–706. [PubMed: 8893026]

20. Komatsu H, Jin YH, L'Etoile N, Mori I, Bargmann CI, Akaike N, Ohshima Y. Functional reconstitution of a heteromeric cyclic nucleotide-gated channel of Caenorhabditis elegans in cultured cells. Brain Res 1999;821:160–168. [PubMed: 10064800]

21. Morton DB. Invertebrates yield a plethora of atypical guanylyl cyclases. Mol Neurobiol 2004;29:97–116. [PubMed: 15126679]

22. van den Akker F, Zhang X, Miyagi M, Huo X, Misono KS, Yee VC. Structure of the dimerized hormone-binding domain of a guanylyl-cyclase- coupled receptor. Nature 2000;406:101–104. [PubMed: 10894551]

23. Baude EJ, Arora VK, Yu S, Garbers DL, Wedel BJ. The cloning of a Caenorhabditis elegans guanylyl cyclase and the construction of a ligand-sensitive mammalian/nematode chimeric receptor. J Biol Chem 1997;272:16035–16039. [PubMed: 9188508]

24. Chang S, Johnston RJ, Frokjaer-Jensen C, Lockery S, Hobert O. MicroRNAs act sequentially and asymmetrically to control chemosensory laterality in the nematode. Nature 2004;430:785–789. [PubMed: 15306811]

25. Chelur DS, Chalfie M. Targeted cell killing by reconstituted caspases. Proc Natl Acad Sci U S A 2007;104:2283–2288. [PubMed: 17283333]

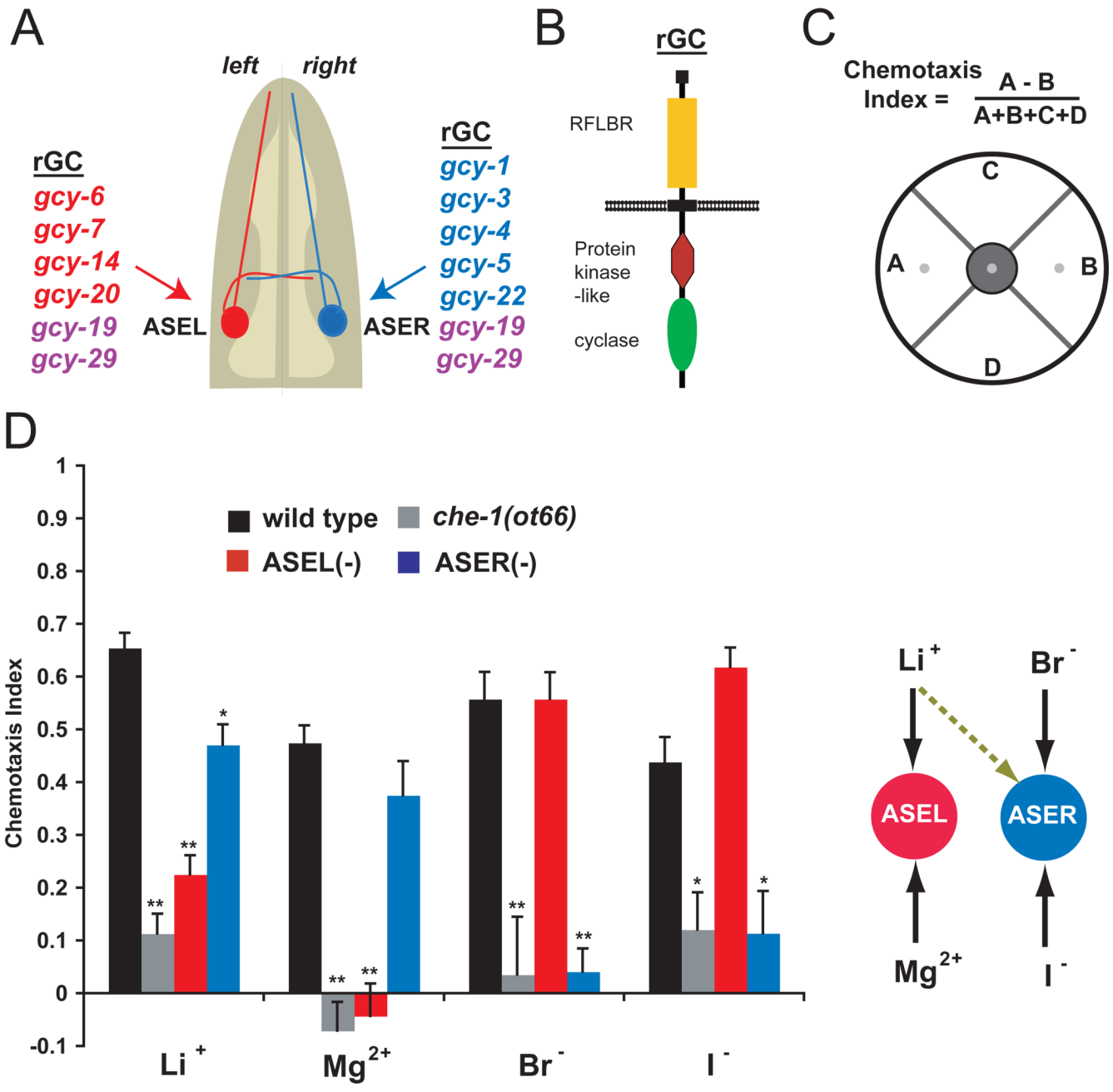

Figure 1. Newly characterized salt taste cues are sensed by ASEL/R in a left-right asymmetric manner

(A) Schematic depiction of the ASE chemosensory neuron pair. In addition to the left/right asymmetrically expressed *gcy* genes shown here (indicated in red for ASEL-expressed and blue for ASER-expressed), ASEL and ASER also express two *gcy* genes (indicated in purple) in a bilaterally symmetric manner [9].

(B) Schematic structure of GCY proteins analyzed in this study. RFLBR = receptor family ligand binding region, a domain present in many, but not all GCY proteins and homologous to bacterial amino acid binding receptors [9].

(C) Schematic of the population chemotaxis assay. Attractant is spotted in quadrant A and a diametrically opposite spot in quadrant B is spotted with water as a negative control.

(D) Population chemotaxis assays of wild-type, *che-1(ot66)*, ASEL-ablated and ASER-ablated worms. Ablations were achieved by cell-specific caspase expression [25]. Each bar represents the mean and standard error of at least four independent assays. Differences between chemotaxis of wild-type and *che-1* or ASEL/R ablated animals were assessed for significance using a two-tailed Student's t-test. Bonferroni correction requires $p < 0.0169$ for significance, which is met in all differences marked as significant ($^*p < 0.01$, $^{**}p < 0.001$). The diagram to the right indicates the ion sensitivities of ASEL and ASER suggested by the ablation data. The dashed gray arrow indicates weak detection by ASER. All assays were done with ammonium or acetate as counterions to individual ions tested with NH_4Ac in the background (see Methods).

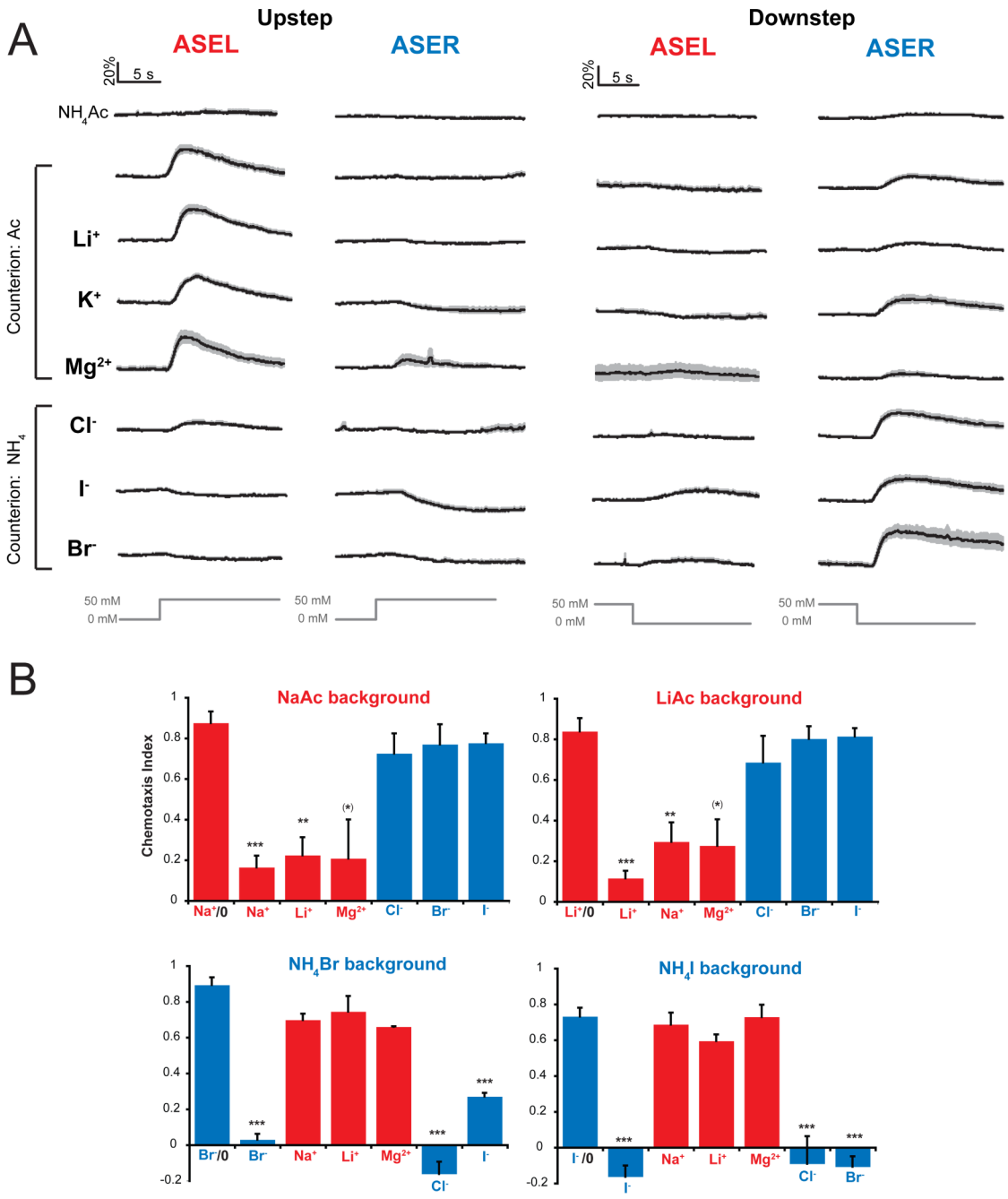

Figure 2. ASEL and ASER are functionally lateralized thereby permitting discrimination of distinct salt cues

(A) Calcium response of ASEL and ASER to concentration steps of various salts. Average calcium transients in response to 50 mM upsteps or downsteps of indicated salts. The grey bands represent ±1 s.e.m.; n = 10 or more recordings, with one recording per worm. Traces represent the average percentage change from baseline over time of the fluorescence emission ratio of the ratiometric calcium sensor cameleon. Supplementary Fig.S4 calculates an asymmetry index for the individual salt responses.

(B) Salt discrimination assays. Chemotaxis of wild-type worms to a gradient of one salt (indicated on the x-axis) in the uniform presence of another salt ion, indicated at the top of

each panel ("salt discrimination assays"). Red indicates ASEL-sensed cues, blue indicates ASER-sensed cues. Ion background concentrations were 100 mM for NH_4Br and NH_4I, and 50 mM for NaAc and LiAc. Not shown is a discrimination assay with Cl^- in the background, which yielded the expected results of preventing Br^- and I^-, but not Na^+, Li^+ and Mg^{2+} attraction. Although saturating background concentrations of Na^+ and Li^+ interfere with Mg^{2+} attraction, a 100 mM background concentration of Mg^{2+} failed to interfere with the response to Na^+ and Li^+ (not shown). Differences between the chemotaxis response of animals in a given set of discrimination assay conditions were compared to the response observed on a gradient of the same salt without a saturating background (*e.g.* in upper left panel, Na^+/Na^+ *vs.* Na^+/0, Li^+/Na^+ *vs.* Li^+/0, *etc*.) using a two-tailed Student's t-test. Bonferroni correction requires $p < 0.0085$ for significance, which is met in all differences marked as significant (*$p < 0.05$, **$p < 0.01$, ***$p < 0.001$). In the case of Mg^{2+} chemotaxis in a Na^+ and Li^+ background, significance was only observed without the Bonferroni correction (star in parenthesis). "0" indicates control assay in which chemotaxis was tested on buffered agar without a saturating salt background. Ions forming gradients are listed on the *x*-axes.

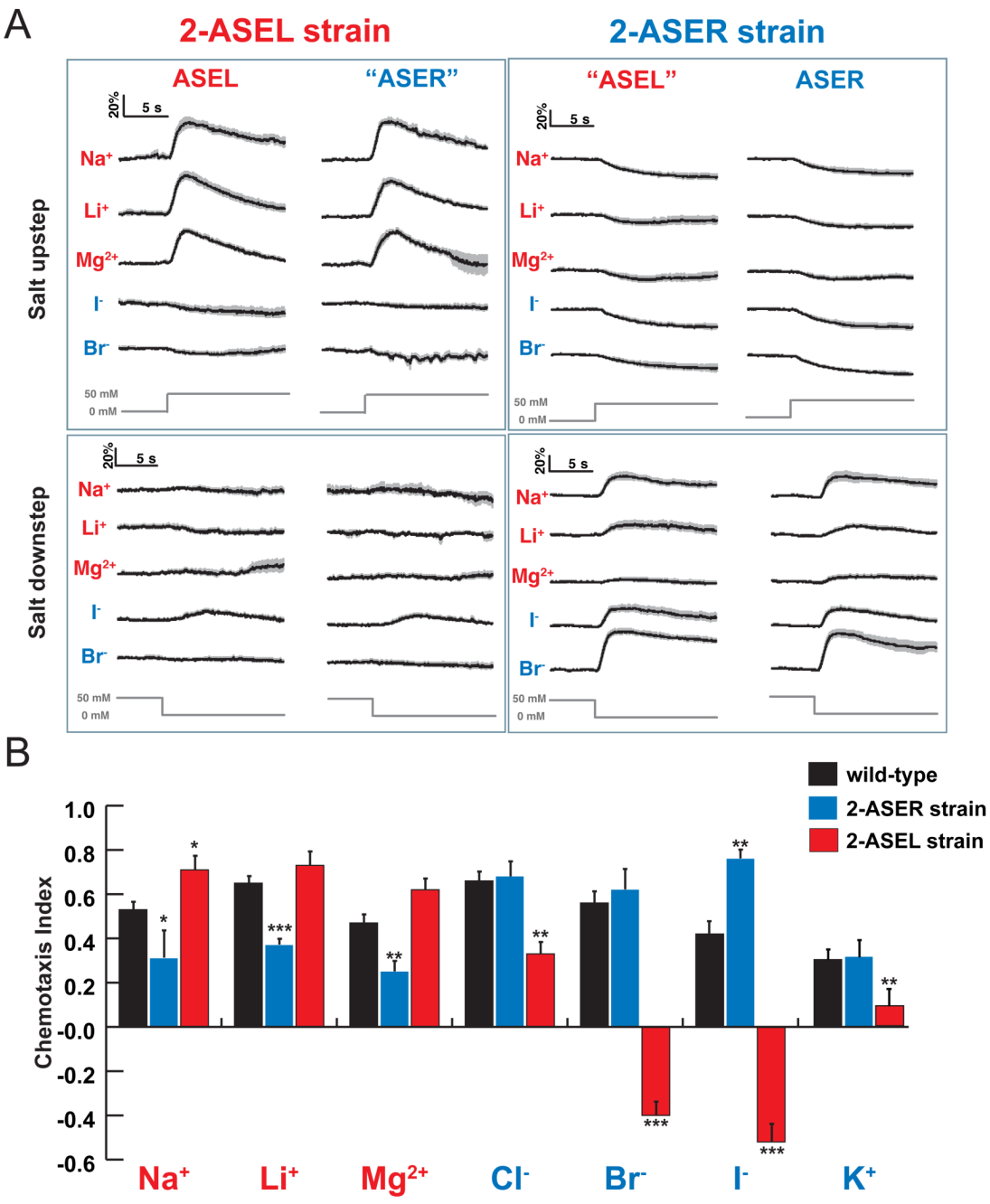

Figure 3. Behavioral and calcium imaging analysis of "2-ASER" and "2-ASEL" asymmetry mutants

(A) Average calcium transients ± s.e.m of left and right ASE neurons in *lsy-6(ot71)* (2-ASER), and *otIs204[ceh-36::lsy-6]* (2-ASEL) animals (n>10), in response to 50 mM upsteps and downsteps of indicated salts. Conditions were as in Fig.2.

(B) Population chemotaxis assays of wild-type, *lsy-6(ot71)* (2-ASER), and *otIs204 [ceh-36::lsy-6]* (2-ASEL) animals. Each bar represents the mean ± s.e.m. of at least four independent assays. Differences between wild-type and experimental conditions were assessed using a two-tailed Student's t-test. Bonferroni correction requires $p < 0.0253$ for significance, which is met in all differences marked as significant (*$p < 0.05$, **$p < 0.01$, ***$p < 0.001$).

Assays were done as shown in Fig.1. Note that “2-ASEL mutants” do not merely show a decrease in response to the ASER cues Br^- and I^-, but are now strongly repelled by these cues; this repulsion depends on ASE, as it is abrogated upon genetic ablation of ASE in a *che-1* mutant background (data not shown).

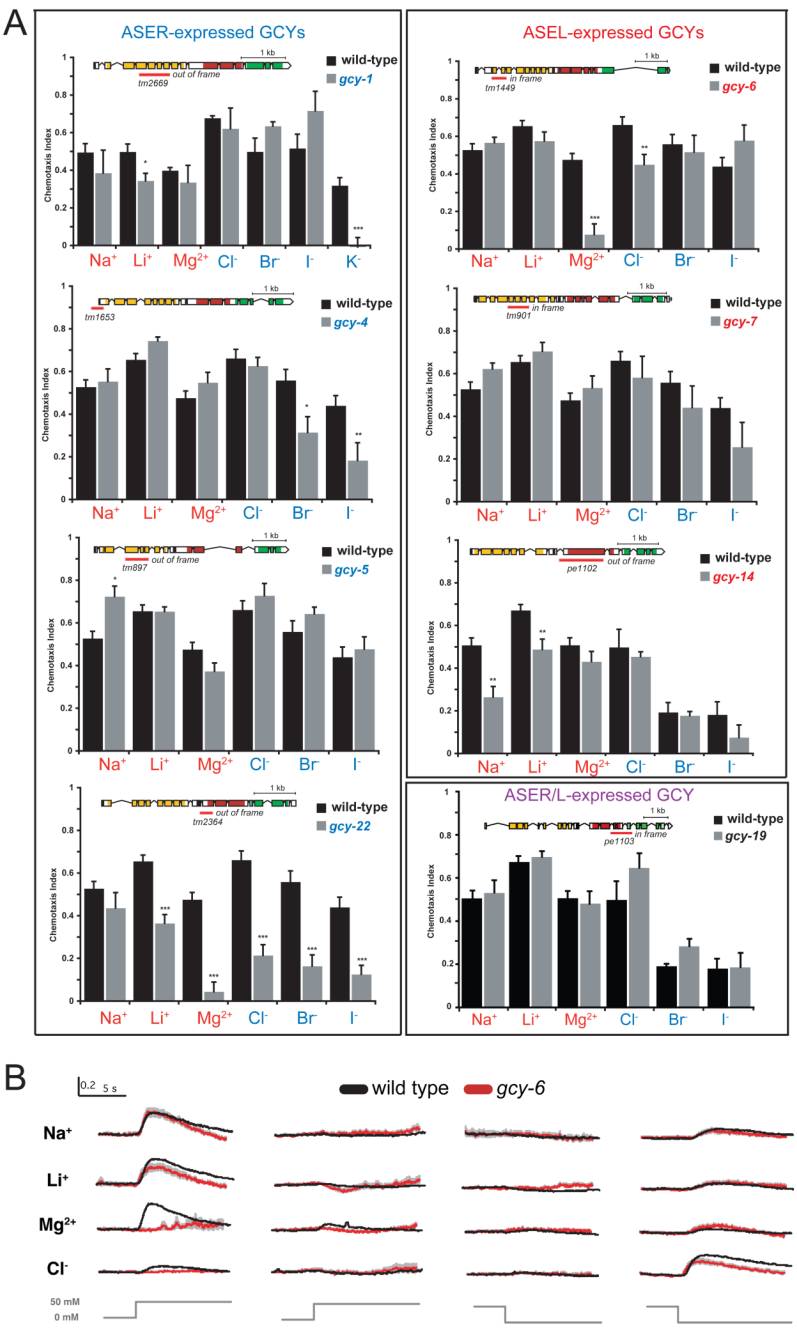

Figure 4. Responses of *gcy* mutant animals to ASE-sensed salts

(A) Chemotaxis assays. Each graph depicts chemotaxis index of wild-type and *gcy* mutant worms on gradients of indicated salts. Assays were done as shown in Fig.1. Wild-type data (and single mutant data in the case of the double mutant analysis) are duplicated in each graph to facilitate side-by-side comparisons, except in those cases were data were collected by different observers. The deletion allele used is shown schematically above each panel; color coding of exons correspond to color coding of rGC protein domains in Fig.1B. Each bar represents the mean ± s.e.m. of at least three independent assays. Differences between chemotaxis of wild-type and mutant strains, or between single and double mutants, were assessed for significance using a two-tailed Student's t-test. Bonferroni correction requires p

< 0.05 for significance, which is met in all differences marked as significant (*p < 0.05, **p < 0.01, ***p < 0.001).

(B) Calcium imaging responses to salt taste cues in *gcy-6* mutants. Calcium responses of wild-type animals (black) are taken from Fig.2 for comparison. n>10. Conditions were as shown in Fig.2.

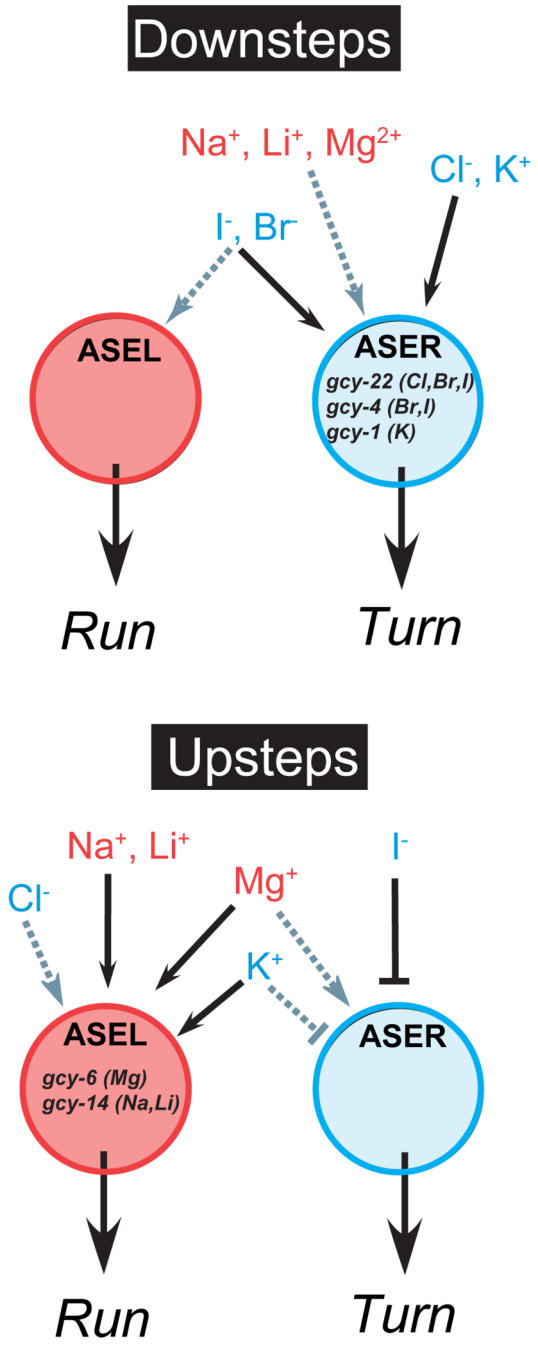

Figure 5. Schematic diagram of asymmetric cellular activation of ASEL/R and behavioral outputs promoted by individual salt taste cues

Color coding of ions indicates ASEL-biased cues (red) or ASER-biased cues (blue) based on ablation data and ASE calcium imaging. Arrows indicate that the salt causes a relatively strong (black) or relatively weak (grey) transient calcium increase in ASEL/R during a downstep/upstep. T-bar indicates that I^- upstep causes a relatively strong transient calcium decrease in ASER. Lists of *gcy* genes within cells summarizes which salt cues are thought to require which *gcy* genes for signaling in that particular cell, based on mutant analysis, *gcy* expression profiles, calcium imaging, and *gcy* cell-specific rescue experiments. Run and turn outputs are based on the findings of Suzuki *et al.* [6].